LA-UR-05-1904

Approved for public release; distribution is unlimited.

Title: 148-Gd Production Cross Section Measurements for 600- and 800-MeV Protons on Tantalum, Tungsten, and Gold

Author(s): K. C. Kelley, N. E. Hertel, E. J. Pitcher, M. Devlin, S. G. Mashnik

Submitted to: Nucl. Phys. A 760 (2005) 225

Available online at www.sciencedirect.com
SCIENCE DIRECT®
Nuclear Physics A 760 (2005) 225–233
NUCLEAR PHYSICS A

^{148}Gd production cross section measurements for 600- and 800-MeV protons on tantalum, tungsten, and gold ☆

K.C. Kelley [a,*], N.E. Hertel [b], E.J. Pitcher [a], M. Devlin [a], S.G. Mashnik [a]

[a] *Los Alamos National Laboratory, Los Alamos, NM 87545, USA*
[b] *Georgia Institute of Technology, Atlanta, GA 30332-0425, USA*

Received 30 March 2005; received in revised form 1 June 2005; accepted 2 June 2005

Available online 24 June 2005

Abstract

The production of ^{148}Gd due to the spallation of tantalum, tungsten, and gold interacting with 600- and 800-MeV protons is investigated. The cumulative ^{148}Gd production cross section was measured using charged-particle spectroscopy at WNR's facility at LANSCE. These data are compared with previous measurements and theoretical predictions of Bertini + Dresner, CEM2k + GEM2, and INCL4-ABLA. The importance of the new data on the reaction models are discussed.
Published by Elsevier B.V.

PACS: 24.10.Lx; 25.40.Sc; 29.30.Eq

Keywords: NUCLEAR REACTIONS, W, TA, Au$(p, X)^{148}$Gd, $E = 600, 800$ MeV; measured cumulative production σ. Comparison with previous results, model predictions.

☆ This work formed part of the PhD thesis of K.C. Kelley at GIT.

* Corresponding author.
E-mail address: corzine@lanl.gov (K.C. Kelley).

0375-9474/$ – see front matter Published by Elsevier B.V.
doi:10.1016/j.nuclphysa.2005.06.002

1. Introduction

Proton accelerators in the energy range of a few hundred MeV to a few GeV are used to produce neutrons in a heavy metal target. The heavy metals tungsten, tantalum, and uranium are currently being used as spallation neutron targets and cladding. Liquid mercury is the proposed target material at the Spallation Neutron Source in the USA, as well as the Japanese Spallation Neutron Source, both of which are planned to come online in the later half of this decade.

Spallation occurs in two main stages, an intranuclear cascade stage followed by an evaporation-fission stage. The intranuclear cascade involves incident particles ($E \gtrsim$ 100 MeV) interacting with individual nucleons, instead of the nucleus as a whole. Several high-energy particles can leave the nucleus and potentially initiate further spallation reactions in neighboring nuclei, resulting in a chain reaction process that eventually dies out when secondary particles no longer have sufficient energy to initiate a spallation event. The nucleus involved in the spallation reaction is left in an excited state and relieves its excitation energy by competing processes of evaporation or fission. If the excitation energy of the residual nucleus produced after the intranuclear cascade stage of a reaction is of the order of tens of MeV or greater, preequilibrium emission of particles is also possible during the equilibration of the nucleus, before evaporation of particles or fission of the compound nucleus.

Simulation of spallation reactions has relied heavily on nuclear reaction models. To date, spallation product yield measurements have been performed using gamma spectroscopy, fragment separators, and radiochemical analysis. One spallation product that has typically not been measured is ^{148}Gd, an alpha emitter with a 75-year half-life. This radionuclide is a large contributor to the dose burden at spallation target facilities. As far as we know, only two measurements of ^{148}Gd production for intermediate energy protons exist. An independent yield using inverse kinematics measured the independent $^{197}\mathrm{Au}(p,x)\,^{148}$Gd production at 800 MeV at GSI [1]. The cumulative yield was then determined by including production from the decay of its radioactive parents. For ^{148}Gd, all of the radioactive parents are less than one hour in half-life. One other measurement for 800 MeV protons on tungsten could be inferred from an internal report on the Accelerator Production of Tritium decay heat experiment at LANSCE [2,3]. The authors measured the cumulative ^{148}Gd production cross section for 600 and 800 MeV protons on tantalum, tungsten, and gold. These measurements are compared with three physics models—the default physics models of MCNPX (Bertini intranuclear cascade, MPM preequilibrium, Dresner evaporation, RAL fission, GCCI level density), referred to herein as "Bertini + Dresner", [4], CEM2k + GEM2 [5,6], and INCL4-ABLA [7–9].

2. Irradiations

A series of irradiations took place during 2002 and 2003 at LANSCE's WNR facility using thin foils. The tantalum, tungsten, and gold foils (>99.9% purity) were nominally 3 μm in thickness so that proton energy loss through a foil was negligible. Aluminum activation foils (10 μm thickness, 99.0% purity) were used for beam monitoring with the

Table 1
Irradiations performed in the Blue Room at WNR during the 2002–2003 run cycle. Each irradiation measured the proton fluence with ^{22}Na activation from Al foils and current monitors upstream of targets

Metal foils	Singles or stacked foils	E_p (MeV)	Time averaged ϕ_p (p/s)		Ratio of ^{22}Na to monitor
			^{22}Na activation	Current monitor	
W, Ta, Au	stacks of 3	600	1.76×10^{13}	1.63×10^{13}	1.08±0.09
Ta	stacks of 3	800	1.42×10^{13}	1.32×10^{13}	1.08±0.05
Au	stacks of 3	800	2.38×10^{13}	2.32×10^{13}	1.03±0.05
W	stacks of 3	800	2.41×10^{13}	2.48×10^{13}	0.972±0.049
W, Ta, Au	singles	800	1.83×10^{13}	1.72×10^{13}	1.06±0.05

well-known ^{27}Al(p, x) ^{22}Na reaction. The reported cross sections of Tobailem's measurement [10], 16.0 ± 1.1 mb at 600 MeV, and of Morgan's [11] at 800 MeV, 14.3 ± 0.4 mb, were used to determine the proton fluence by counting the ^{22}Na with a HPGe detector calibrated with a ^{152}Eu source.

Stacks of three foils of the same heavy metal were irradiated at 600 MeV and 800 MeV for one set of measurements. In these measurements, only the middle foil was counted, assuming recoils gained from the first foil balanced the loss of recoils to the third foil. Another irradiation performed at 800 MeV used single heavy metal foils sandwiched between two aluminum "catcher" foils. In this case, the sum of ^{148}Gd alphas detected from the heavy metal foil and the two aluminum catcher foils were used to determine the production cross section. This approach was viable because ^{148}Gd is not produced by spallation reactions in Al. The counting of the catcher foils corrects for any recoils from the heavy metal foil. The portion of ^{148}Gd recoiling forwards and backwards could also be determined by this method.

During these irradiations, current monitors upstream of the target were recorded every second. These current monitor readings (3% uncertainty) are compared with the measured ^{22}Na activation from the aluminum foils (7.7% uncertainty at 600 MeV and 4.1% uncertainty at 800 MeV) in Table 1. The proton fluence measured from ^{22}Na activation level was within 8% of the current monitor, although generally higher, lending confidence in the reaction cross sections used. Higher reliability was given to the ^{22}Na measurements since these were direct measurements at the location of the foil irradiations. The current monitors were located approximately 6 m upstream of the irradiation site. In this distance, proton loss could have occurred due to spray in the beam.

3. Measurements

As ^{148}Gd decays, the nuclide emits a 3.18-MeV α particle. These α's were measured using silicon charged-particle detectors in vacuum ($\sim$1 torr). No other radionuclide with decay α energy less than 3.5 MeV could be detected because of their short ($<$1 day) or long ($<10^6$ yr) half-lives or their low probability of alpha decay ($<10^{-3}$%). The efficiency of the system was determined using calibrated ^{148}Gd and ^{241}Am sources. The efficiency curve was essentially linear with respect to energy for the charged-particle detection system.

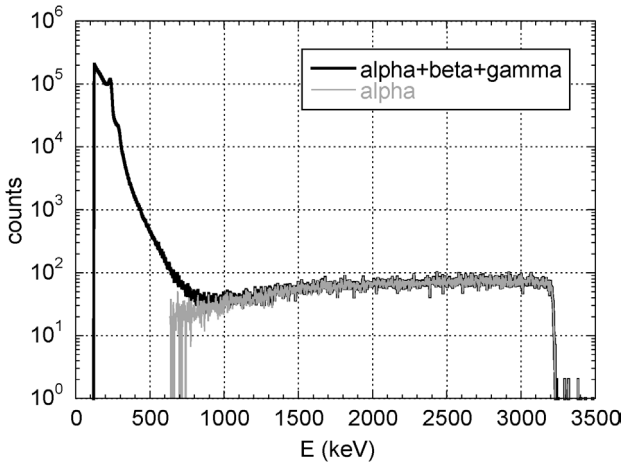

Fig. 1. Charged particle spectrum of foil W7 (3.6 μm thin) from the 800-MeV stacked foil irradiation. The alpha + beta + gamma spectrum was directly measured while the alpha spectrum was obtained by subtracting the beta + gamma background from the alpha + beta + gamma spectrum. Counting time was 3 days.

The range of a 3.2-MeV α particle in tungsten and gold (19.3 g/cm^3) is 4.76 μm, while a 3 μm thickness corresponds to an energy loss of 1.7 MeV [12]. Assuming ^{148}Gd was produced uniformly through 3 μm foils, a broad alpha peak ranging from ∼1.5 to 3.2 MeV was expected. Because tantalum has a lower density (16.6 g/cm^3), a broad peak was expected from ∼1.8 to 3.2 MeV. The aluminum foil thickness (10 μm) selected was thicker than the heavy metal foils, since the α particle range is longer in aluminum (2.7 g/cm^3).

A wide energy range of beta and gamma particles from various radionuclides were also emitted from the foils and detected. Only low energy electrons deposited all of their energies in the detector. Higher energy electrons deposited only a portion of their energy. This complicated the alpha counting since the lower energy portion of the alpha peak was superimposed on the beta + gamma background for the tungsten and gold foils. This problem was solved by placing a thin aluminum foil in front of the irradiated foil to block all the alphas from reaching the detector. The beta + gamma spectrum was then subtracted from the combined alpha + beta + gamma spectrum to produce a clean alpha peak (Fig. 1).

The cumulative ^{148}Gd production cross sections presented in Table 2 are measurements for 600 and 800 MeV protons on tantalum, tungsten, and gold. The stacked foil measurements compared well within 1σ of the single foil measurements. The ^{148}Gd recoils adhering to the aluminum foils were 10% of the total ^{148}Gd measured, with the forward recoils contributing 90–95% of the total recoils. The uncertainties of the measured yields vary from 11% to 26% at 600 MeV and from 6% to 25% at 800 MeV. Goodfellow Corporation, which made the foils, reported a nominal uncertainty of 25% in the thickness of the foils, which originally dominated the uncertainty in the cross sections. To reduce this uncertainty, X-ray fluorescence was used to map out the relative thickness pixel-by-pixel over the area of the irradiated foils. The array was then normalized by the average thickness (measured by weight and size prior to the irradiations) and weighted by the proton fluence profile obtained from radiographic imaging after the irradiation. This analysis was

Table 2
Cumulative ^{148}Gd production cross section measurements

Target	Energy (MeV)	Foil setup	Cross section (mb)
Ta	600	stacked	15.2 ± 4.0
	800	stacked	29.7 ± 7.6
		single	27.6 ± 1.7
		single	28.6 ± 7.3
W	600	stacked	8.31 ± 0.92
	800	stacked	19.5 ± 1.2
		single	18.0 ± 1.1
		single	20.7 ± 5.3
Au	600	stacked	0.591 ± 0.155
	800	stacked	3.86 ± 0.98
		single	3.52 ± 0.22

performed on three tungsten foils, one tantalum foil, and one gold foil to reduce the total uncertainties in their yields to 11% at 600 MeV and 6% at 800 MeV. Further details on the uncertainty analysis can be found in [13].

4. Theoretical predictions

For each of the codes used to compute the ^{148}Gd production cross section, the default options were chosen to give a general comparison. The defaults of Bertini + Dresner and INCL4-ABLA were as implemented in MCNPX version 2.5.e. The version of CEM2k + GEM2 used supersedes the version of CEM included in release 2.5.e of MCNPX. The independent yields for ^{148}Gd and all of its radioactive parents were computed and summed to determine a cumulative yield. The differences between the codes' values are as much

Table 3
Comparison of independent radionuclide yields used in calculating the cumulative ^{148}Gd yield from 800-MeV protons on tungsten

	% contrib. to cumul.	Independent cross section (mb)		
		Bertini + Dresner	CEM2k + GEM2	INCL4-ABLA
^{148}Gd	100	9.26 ± 1.58	4.65 ± 0.14	2.26 ± 0.06
^{148}Tb	100	5.59 ± 0.13	6.98 ± 0.17	3.92 ± 0.08
^{148}Dy	100	3.28 ± 0.10	12.9 ± 0.2	2.50 ± 0.06
^{148}Ho	100	0.003 ± 0.003	0.812 ± 0.058	0.388 ± 0.025
^{152}Dy	0.1	13.9 ± 0.19	8.17 ± 0.18	6.47 ± 0.10
^{152}Ho	23.0	4.87 ± 0.12	9.56 ± 0.20	6.93 ± 0.11
^{152}Er	91.2	1.72 ± 0.07	13.7 ± 0.2	2.55 ± 0.06
^{152}Tm	91.2	0.003 ± 0.003	0.428 ± 0.042	0.184 ± 0.017
^{156}Tm	0.007	3.08 ± 0.09	7.07 ± 0.17	7.50 ± 0.11
^{156}Yb	9.13	0.455 ± 0.035	9.52 ± 0.20	1.53 ± 0.05
^{156}Lu	86.6	0.000 ± 0.000	0.093 ± 0.019	0.039 ± 0.008
^{160}Hf	0.064	0.011 ± 0.005	1.11 ± 0.07	0.445 ± 0.027
Cumulative		20.9 ± 1.6	41.4 ± 0.4	13.3 ± 0.1

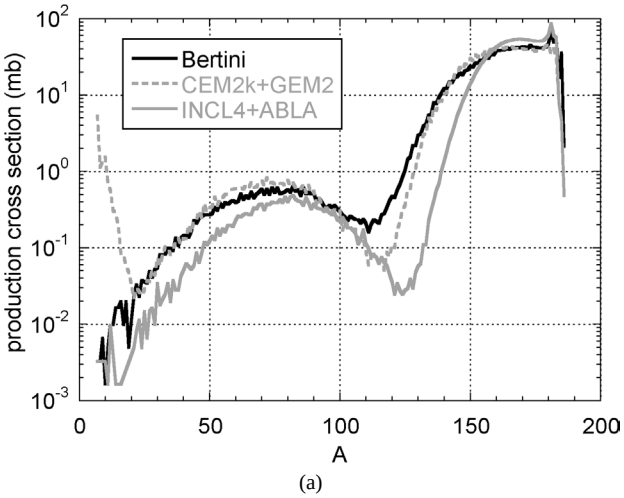

(a)

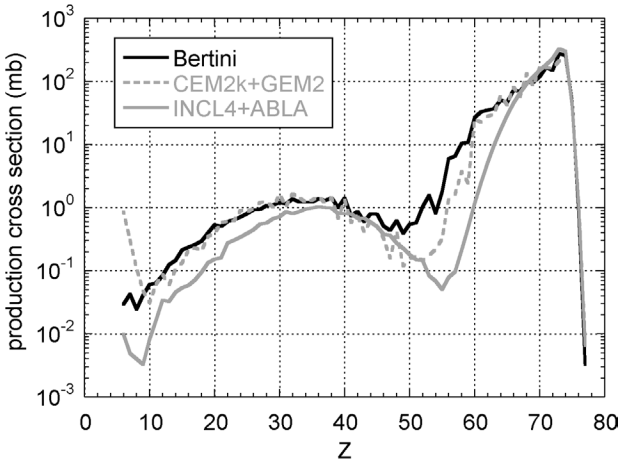

(b)

Fig. 2. Production cross section curves of 800 MeV p + W for Bertini + Dresner, CEM2k + GEM2, and INCL4-ABLA as a function of (a) mass and (b) charge.

as an order of magnitude different for the independent yields and a factor of three for the cumulative yields (Table 3).

The spallation production cross sections in Fig. 2 illustrate the differences between the codes predictions for 800 MeV protons on tungsten. These data indicate that ^{148}Gd is produced entirely by evaporation, with little to no contribution from fission. To further see how these codes compare, mass and charge distributions of the product yields are shown for individual charge numbers 64 to 72 in Fig. 3. The radionuclides listed in Table 3 are not the most probable nuclides that would be produced by the spallation process according to Fig. 3. Instead, these radionuclides are among the lower yield nuclides making their yields difficult to predict.

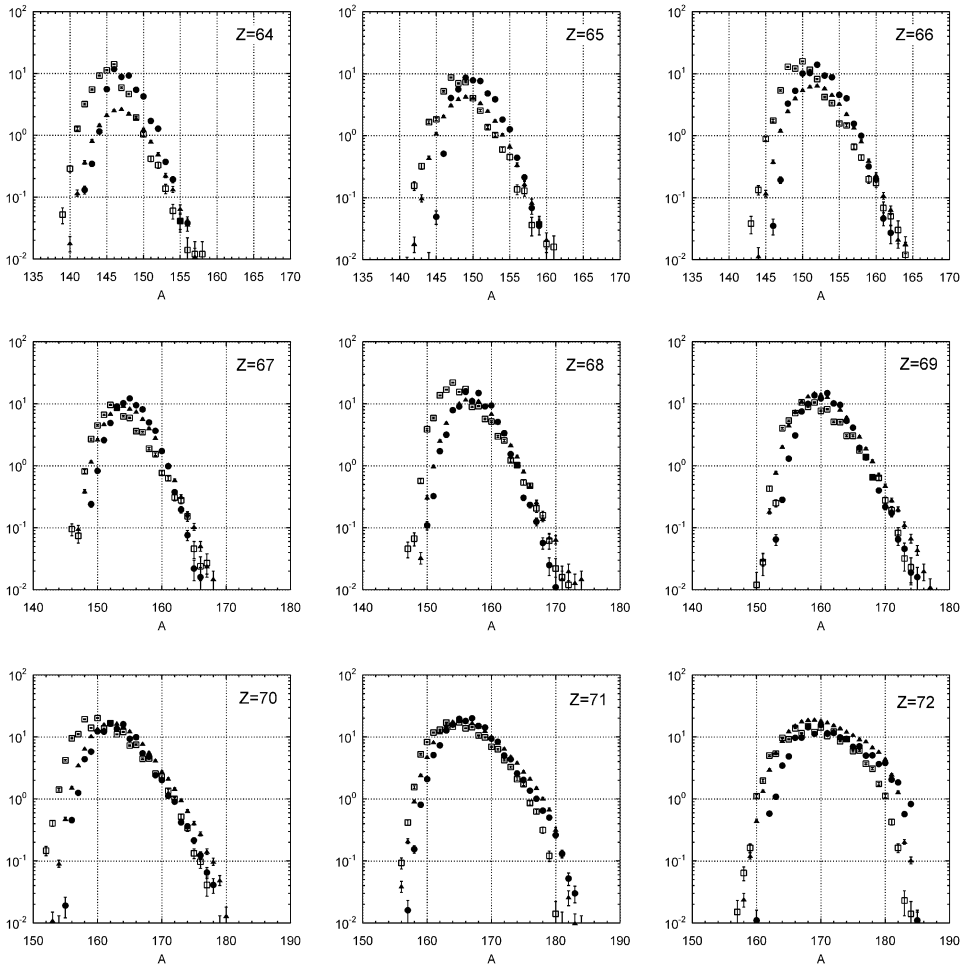

Fig. 3. Independent radionuclide production curves from 800 MeV protons incident on tungsten for $Z = 64$ to 72. Open squares represent CEM2k + GEM2, filled circles represent Bertini + Dresner, and filled triangles represent INCL4-ABLA.

5. Comparison of measurements and predictions

The measurements in Table 2 were averaged together to produce a single cross section measurement for a particular target and energy. These measurements are compared with previous measurements and theoretical predictions in Table 4. The average value of the current measurement for ^{148}Gd yield from W at 800 MeV was well within 2σ of the previous measurement by Henry [2] and the average for Au at 800 MeV was in perfect agreement with the previous measurement by Rejmund [1]. The Bertini + Dresner approach better predicted the ^{148}Gd production than the CEM2k + GEM2 and INCL4-ABLA algorithms. Bertini + Dresner yields ranged from 2–25% of the measurement values for Ta and W

Table 4
Summary of cumulative ^{148}Gd production cross section measurements and comparisons to theoretical predictions and previous measurements

Target	E_p (MeV)	^{148}Gd cumulative production cross section (mb)				
		Measurements		Theoretical		
		This work	Previous work	CEM2k + GEM2	Bertini + Dresner	INCL4-ABLA
Ta	600	15.2 ± 4.0		29.4 ± 0.2	15.5 ± 0.2	6.23 ± 0.09
	800	28.6 ± 3.5		45.6 ± 0.3	24.4 ± 0.3	17.3 ± 0.2
W	600	8.31 ± 0.92		21.6 ± 0.3	10.9 ± 0.2	4.21 ± 0.08
	800	19.4 ± 1.8	16.4 ± 0.8 [2]	41.4 ± 0.4	20.9 ± 0.2	13.3 ± 0.1
Au	600	0.591 ± 0.155		1.41 ± 0.04	0.929 ± 0.049	0.036 ± 0.007
	800	3.69 ± 0.50	3.74 ± 0.19 [1]	12.9 ± 0.1	7.23 ± 0.14	0.596 ± 0.029

and 35–50% higher than the Au measurements. The CEM2k + GEM2 predictions were a factor of two to three higher than the measurements while the INCL4-ABLA predictions were a factor of two lower than the measurements for Ta and W and an order of magnitude lower for Au. The comparisons to the measurements for all three codes were best for Ta and W and worst for Au. This is reasonable since Ta is closer in nucleon number to Gd and therefore it is easier to predict ^{148}Gd from the spallation of Ta.

6. Conclusion

The cumulative ^{148}Gd production cross section was measured for 600- and 800-MeV protons on tantalum, tungsten, and gold using charged-particle spectroscopy of foils. These measurements compare well with previous measurements for tungsten and gold at 800 MeV, which used different techniques. All of the yield predictions were within a factor of two to three for the Bertini + Dresner and CEM2k + GEM2 models. The predictions from INCL4-ABLA were within a factor of two to three for tungsten and tantalum and an order of magnitude off for gold.

Acknowledgements

The authors would like to acknowledge Dr. Sylvie Leray for her useful discussions. This study was supported by the US Department of Energy under contract W-7405-Eng-36 with the University of California.

References

[1] F. Rejmund, B. Mustapha, P. Armbruster, J. Benlliure, M. Bernas, A. Boudard, J.P. Dufour, T. Enqvist, R. Legrain, S. Leray, K.-H. Schmidt, C. Stéphan, J. Taieb, L. Tassan-Got, C. Volant, Nucl. Phys. A 683 (2001) 540.

[2] E.A. Henry, K.J. Moody, unpublished report.
[3] D.L. Quintana, R.L. Barber, M.J. Baumgartner, R.D. Brown, J.N. Edwards, B.A. Faulkner, T.L. Figueroa, J.J. Jarmer, R. Kidman, P.D. Olivas, M.A. Paciotti, L.S. Waters, R.D. Werbeck, G.J. Wilcutt, K.A. Woloshun, in: Proceedings of 4th International Topical Meeting on Nuclear Applications of Accelerator Technology, Washington, DC, 12–15 November, 2000, p. 405.
[4] L.S. Waters (Ed.), LA-CP-02-408.
[5] S.G. Mashnik, A.J. Sierk, K.K. Gudima, LA-UR-02-5185, in: 12th Biennial Topical Meeting of the Radiation Protection and Shielding Division of the American Nuclear Society, Santa Fe, NM, 14–17 April, 2002, nucl-th/0208048.
[6] S.G. Mashnik, K.K. Gudima, A.J. Sierk, in: Proceedings of the 6th Int. Workshop on Shielding Aspects of Accelerators, Targets and Irradiation Facilities (SATIF-6), Stanford Linear Accelerator Center, CA, 10–12 April, 2002, LA-UR-03-2261, nucl-th/0304012.
[7] A. Boudard, J. Cugnon, S. Leray, C. Volant, Phys. Rev. C 66 (2002) 044615.
[8] J.J. Gaimard, K.-H. Schmidt, Nucl. Phys. A 531 (1991) 709.
[9] A.R. Junghans, M. de Jong, H.-G. Clerc, A.V. Ignatyuk, G.A. Kudyaev, K.-H. Schmidt, Nucl. Phys. A 629 (1998) 635.
[10] J. Tobailem, CEA-N-1466(5).
[11] G.L. Morgan, K.R. Alrick, A. Saunders, F.C. Cverna, N.S.P. King, F.E. Merrill, L.S. Waters, A.S. Carroll, A.L. Hanson, R.P. Liljestrand, R.T. Thompson, E.A. Henry, Nucl. Instrum. Methods B 211 (2003) 297.
[12] J.F. Ziegler, J.P. Biersack, U. Littmark, The Stopping and Range of Ions in Solids, Pergamon Press, New York, 1985, http://www.srim.org.
[13] K.C. Kelley, PhD thesis, Georgia Institute of Technology, 2004, http://etd.gatech.edu/theses/available/etd-03292004-191344/.